Error analysis of satellite-based global navigation system over the low-latitude region

G. Sasibhushana Rao

The effect of changes in the environmental conditions surrounding an airport on ground-based navigational aids, such as Doppler very high frequency omni range, distance measuring equipment and instrument landing system course structure, is a major issue that affects the performance of these equipment. Due to the limitations of the ground-based navigational aids, the International Civil Aviation Organization has established a special committee on the Future Air Navigation System (FANS) to look into the development of satellite-aided communication, navigation and surveillance system. The FANS committee concluded that satellite technology was the solution to overcome the shortcomings of ground-based systems and to meet the future needs of the international civil aviation community. Global Positioning System (GPS) is one such system, which is an all-weather satellite-based positioning system funded by the Department of Defence, USA and is available to users anywhere on the globe for various applications, including civil aviation. However, the performance of stand-alone GPS does not meet the Cat-I PA requirement due to several errors. Therefore, for aviation users in the Indian subcontinent, augmentation of GPS is planned through a regional satellite-based augmentation system called GPS-aided geo augmentation system. However, over the Indian subcontinent the ionospheric effects are severe and erratic due to equatorial anomaly. Total electron content variations have been analysed for several years in the low-latitude region. GPS signal structure, various errors affecting the positional accuracy of GPS and the techniques used to mitigate their affects are presented in this article.

Keywords: Error analysis, global navigation system, ionosphere, troposphere.

IN the Tenth Air Navigation Conference held in 1991, the International Civil Aviation Organization (ICAO) established a special committee on Future Air Navigation System (FANS) to look into the development of Satellite-Aided Communication, Navigation and Surveillance (SACNS) system. The present Communication Navigation and Surveillance (CNS) system suffers from propagation limitations of current line of sight system, and accuracy and compatibility between CNS systems in different parts of the world. The new system should be such that it will have universal accessibility to air navigation safety communications from harmful interferences. To realize these objectives effectively, a satellite-based navigation system is needed. Navigation Satellite Timing And Ranging Global Positioning System (NAVSTAR GPS) is one such system. GPS is an all-weather, line-of-sight radio navigation and positioning system. It was developed primarily for military purpose. The multi-purpose usage of NAVSTAR GPS has developed enormously in the last three decades. The system became fully operational[1] in 1994. Currently, there are 29 operational satellites in the constellation. For aviation users in the Indian subcontinent, augmentation of GPS is planned through regional Satellite-Based Augmentation System (SBAS), called the GPS Aided Geo Augmented Navigation (GAGAN). Indian Space Research Organization (ISRO) and Airports Authority of India (AAI) signed an MoU in 2001 to develop and implement GAGAN jointly. Over the low-latitude region (±15° from the geomagnetic equator), ionospheric error is the most predominant one that limits the performance of the satellite-based navigation system. Ionospheric error is a function of Total Electron Content (TEC). TEC variations against the local time and the geomagnetic latitude over the Indian subcontinent are presented by processing the data acquired from dual-frequency GPS receivers located at Hyderabad and the Indian Institute of Science, Bangalore.

GPS satellite signals

The satellites transmit two spread-spectrum pseudorandom noise (PRN) radio signals. The signals consists of a C/A

G. Sasibhushana Rao is in the Department of Electronics and Communication Engineering, Andhra University Engineering College, Visakhapatnam 530 003, India. e-mail: sasi_gps@yahoo.co.in

(coarse acquisition) code at 1.023 MHz and a P- (precision) code at 10.23 MHz bandwidths. The signals are transmitted at two frequencies, L_1 (1575.42 MHz) and L_2 (1227.60 MHz). Both are coherently derived from highly stable on-board atomic clocks. Both C/A and P-codes are transmitted on the L_1 frequency, whereas either C/A or P-code is transmitted on the L_2 frequency depending on the ground command[2]. The C/A code is available to all users; however the P-code is available to only authorized users because of the antispoofing feature. In addition to the PRN range codes, 50-bps data, which consist of the navigation message comprising both ephemeris and clock parameters are modulated onto the PRN sequence on both L_1 and L_2 frequencies. Each GPS satellite transmits its identity number and orbital ephemeris correction in addition to other data such as health, clock errors, drift rates, etc.

Currently, the GPS satellite constellation consists of 29 satellites in near-circular orbits, approximately 20,150 km above the earth. These are positioned in six earth-centred orbital planes with minimum four satellites in each plane. Each satellite is identified with a two-character code: a letter identifies the orbital plane (A through F), and a number identifies the satellite slot in the plane (1 through 4). The orbits are equally spaced above the equator at a 60° separation, with an inclination relative to the equator of nominally 55°. The GPS satellites travel with a velocity of 3.9 km/s. The advantage of greater altitude is that the orbits will be less affected by the irregularities caused by unequal distribution of mass in the earth. Satellite Vehicles (SVs) are arranged such that observers anywhere on the earth's surface will always have at least four satellites in view. The nominal orbital period of a GPS satellite[3] is one-half of a sidereal day or 11 h 58 min.

Errors in fixing the GPS position

The GPS error sources can be classified into three groups (Table 1).

Some of these errors can be estimated and corrected, and some are common to users in a given area of operation. Major error sources are described as follows:

SV clock errors

Individual SV clocks, although highly stable, may deviate from the GPS system time. Even though the navigation message transmitted by the SV contains the corrections towards the clock drifts, there are certain uncorrected clock deviations which cause errors in the pseudo-range estimates.

Ephemeris errors

To compute the pseudo range of the user with respect to a satellite, the user should know the position of the satellite. This information is transmitted by the satellite as part of the navigation message. The position of the satellite is a dynamic one and is influenced by gravitational field and solar pressure. Estimation of the position by a ground master control station is subject to errors due to clock drifts and processing delays in the monitoring stations. The estimated positions of the satellites are uploaded periodically to the respective ones. Errors in the estimation of the satellite position result in the pseudo-range errors and are to be corrected at the user level.

Multipath

The carrier wave propagates along an almost straight line, even though there are small bending effects due to the presence of the atmosphere. Multipath is caused by extraneous reflections from nearby metallic objects, ground or water surfaces reaching the antenna. This has a number of effects: it may cause signal interference between the direct and reflected signal leading to noiser measurement; or may confuse the tracking electronics of the hardware, resulting in a biased measurement that is the sum of the satellite-to-reflector distance and the reflector-to-antenna distance[4]. The theoretical maximum multipath bias that can occur in pseudo-range data is approximately half the code chip length or 150 m for C/A code ranges and 15 m for P-code ranges. Typical errors are much lower (gener-

Table 1. GPS error budget (Hoffmann-Wellenhof *et al.*[3])

Error source	Effect	Description of error	Error budget (1σ error) (m)
Satellite	Clock bias	Errors in the transmitted clock	2.1
	Orbital errors	Errors in the transmitted location of the satellite	2.1
Signal propagation	Tropospheric delay	Errors in the corrections of pseudorange caused by tropospheric effects	0.7
	Ionospheric delay	Errors in the corrections of pseudorange caused by ionospheric effects	4.0
Receiver	Clock bias	Errors in the receiver's measurement of range caused by receiver clock error, thermal noise, software accuracy	0.5
	Multipath	Errors caused by reflected signals entering the receiver antenna	1.4

ally <10 m). The carrier phase multipath does not exceed about ¼λ (5–6 cm) for L_1 and L_2.

Receiver clock offset

GPS receivers are usually equipped with quartz crystal oscillators, which have the following advantages: they are small, consume little power and are relatively inexpensive. In addition, quartz crystal oscillators have good short-term frequency (or time-keeping) stability. The clock offset, usually in the range of several thousands of nanoseconds with regard to the GPS time, is treated as an unknown parameter together with the three coordinate components. By making differencing between satellite observations the receiver clock error can be removed[5].

Tropospheric delay error

The transmitted GPS signal travels through the atmosphere layers before it is received by the antenna of the GPS receiver. The atmosphere consists of two main regions: the troposphere and the ionosphere. The troposphere layer is a neutral part of the atmosphere, which causes attenuation, delay and short-term variations (scintillation) of the GPS signals. The magnitude of the tropospheric delay errors depends on temperature, atmosphere pressure, and partial pressure of water vapour. The magnitude of delay errors is highly correlated with the satellite elevation angles, where it increases significantly with lower elevation angles. The tropospheric delay is the sum of dry and wet components. It can be expressed mathematically as follows:

$$d_{\text{trop}} = d_{\text{dry}} m_{\text{dry}} + d_{\text{wet}} m_{\text{wet}},$$

where d_{trop} is the total tropospheric delay, d_{dry} and d_{wet} the dry delay and wet delay respectively, at zenith, and m_{dry} and m_{wet} the corresponding mapping factors to map the zenith delay to the slant direction of satellite–receiver line of sight.

The dry component contributes approximately 80–90% of the total tropospheric delay and it can be accurately estimated, while the wet component contributes 10–20% of the delay. The wet component is difficult to estimate due to the unpredictable nature of atmospheric water vapour. The dry delay at the zenith[6] is about 2.3 m, while the wet delay is approximately 1–80 cm. The troposphere layer is a non-dispersive medium for GPS frequencies, which means that the tropospheric range errors cannot be cancelled through the use of dual-frequency GPS measurements, unlike the ionospheric delay. The tropospheric range delay can be estimated using a number of models[7,8]. The dry delay can be estimated[9] with an accuracy of less than 1%, while the wet part can only be estimated with an accuracy of 10–20%.

Ionospheric delay error

The second region of the atmosphere is the ionosphere, which extends approximately 50–1500 km above the surface of the earth. The ionosphere is an ionized layer consisting of ions and electrons. In this region the group and phase velocities are not the same as the velocity of light. This fact introduces an ionospheric range delay error. This delay has an equal magnitude and opposite sign for the pseudorange and carrier phase measurements. In addition to the range delay error, there are other effects of the ionosphere on GPS signals such as range-rate errors, and phase and amplitude scintillations. The fact that the ionosphere is a dispersive medium, unlike the troposphere, allows correction of the first-order ionospheric range delay errors. These errors can be evaluated by integrating the electron density along a 1 sq. m column along the signal path using the following equation[10]:

$$d_{\text{ion}} = \frac{40.3}{f^2}\text{TEC}, \tag{1}$$

where f is the signal frequency, and TEC is the total electron content along the signal path. Calculation of absolute TEC is presented in eq. (2) for the case where range measurements are available on two separate frequencies.

$$\text{TEC} = \frac{1}{40.3}\left(\frac{1}{f_1^2} - \frac{1}{f_2^2}\right)^{-1} \text{TEC}(P_1 - P_2)\ \text{el/sq. m}, \tag{2}$$

where f_1 and f_2 are the L_1 and L_2 signal frequencies respectively, P_1 and P_2 the pseudoranges observable on L_1 and L_2 signals, and el is the number of electrons.

Typical magnitudes of the range delay error are a few metres to tens of metres[10], and vary according to several factors such as user location, elevation angle, time of the day, time of the year and solar cycle.

Using a dedicated TURBOROGUE dual-frequency GPS receiver at the National Geophysical Research Institute (NGRI), Hyderabad, India, several days of navigation and observation data in RINEX format were collected and analysed. The navigation data file consists of 38 parameters. However, in our calculations only 23 parameters are used. Navigation data are available for every 2 h. In-between data are generated using the standard formulae. The observation data file consists of C/A, P_1 and P_2 pseudoranges, and L_1 and L_2 phases. Similarly, it includes several other parameters such as satellite PRN number, the number of satellites visible at each epoch, GPS time, satellite health and user location in ECEF frame for all the visible satellites. From this information, satellite position, elevation and azimuth angle of satellite, IPP local time (LT), geomagnetic subionospheric point latitude (IPP latitude, ϕ_m), slant factor, ionospheric time delay and slant TEC for all the visible satellites are estimated.

Example

The local time is calculated using eq. (3) given below

$$\mathrm{LT} = (\lambda_i/15) + \mathrm{UTC}, \tag{3}$$

where UTC is the Universal Time Coordinate, and λ_i the geographic subionospheric point longitude in radians, given by

$$\lambda_i = \lambda_{gg} + \psi \frac{\sin(A_z)}{\cos(\phi_i)}, \tag{4}$$

where λ_{gg} is the reference station geodetic coordinate (longitude), A_z the satellite azimuth, ψ the earth centre angle, and ϕ_i the geographic latitude of subionospheric point in radians, given by

$$\phi_i = \phi_{gg} + \phi \cos(A_z), \tag{5}$$

where ϕ_{gg} is the reference station geodetic coordinate (latitude).

For a given set of geodetic coordinates, $\phi_{gg} = 21.431929°$, $\lambda_{gg} = 84.047724°$, $A_z = -75.975°$, earth centre angle = 15.43° and UTC = 10 h. λ_i and LT are calculated as –2.25098° and 36540 s respectively.

Equivalent vertical TEC versus IPP LT, and geomagnetic latitude (ϕ_m) for one day (19–20 May 1998) are shown in Figures 1 and 2 respectively, for SV-21. This particular satellite is visible from 1300 to 2000 h. As expected, the profiles of the two days differ slightly due to the random nature of the ionosphere. From Figure 1, it is obvious that the TEC is large during the afternoon and reaches a minimum during night-time. The profile in Figure 2 represents TECu with respect to ϕ_m, and is an indication of the path of the SV. The SV travelled 7°–11° and then to 0° latitude. Generally, we expect relatively high TEC values at low-latitude regions. One of the reasons for having relatively high TEC at 8° than at 0° could be due to electrojet effect, which is common in the Indian subcontinent. The GPS satellite signals passing through these IPP latitudes at different local times may be the other reason.

The values of vertical TEC (Figures 1 and 2) in the range 10–70 TECu were derived on 19 May 1998, which is nearer to the solar maximum year. At solar maximum year 2000, these values are observed to be in the high range (70–100 TECu). The dual-frequency GPS receiver data collected from Hyderabad and the maximum delay observed on 3 December 2000 for satellite no. 7 is 77.87 m at the GPS L_1 frequency (Figure 3).

The differences between the measurements made at the same local time are attributed to the ionospheric TEC gradients encountered by satellite paths intersecting the ionosphere at different latitudes. It is obvious from Figure 3 that the peaks occur at different timings of the day.

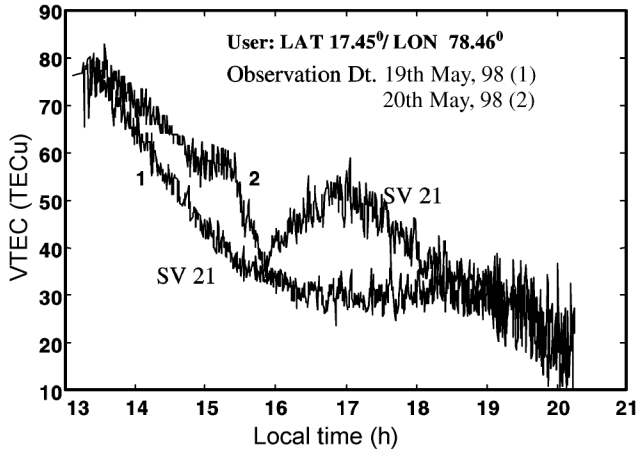

Figure 1. Local time vs VTEC.

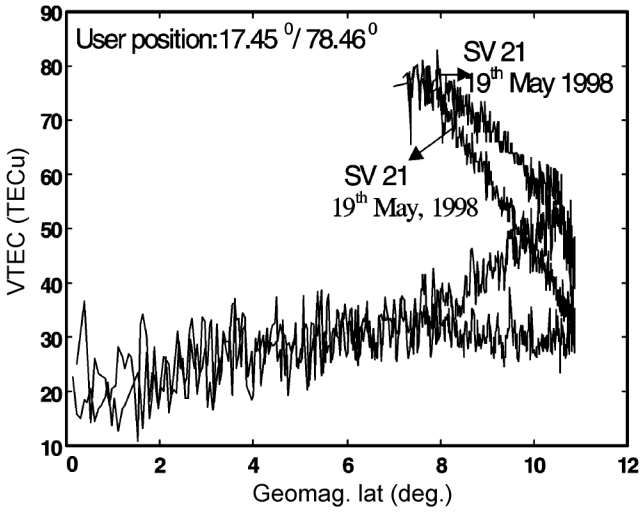

Figure 2. Geomagnetic latitude vs VTEC.

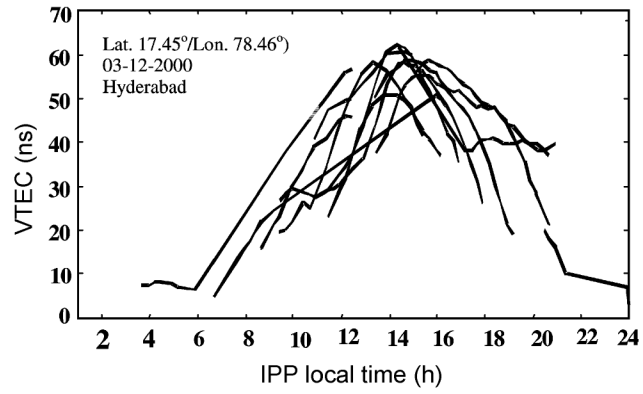

Figure 3. Time delay vs ionospheric local time for all visible satellites.

Need for modernization of GPS

Presently, stand-alone GPS civilian users have access only to C/A-code on L_1. Because of this, they cannot make a dual-frequency ionospheric delay correction. The other major problems are:

(i) L_1 and L_2 signals are not afforded total spectrum protection and they are relatively weak due to background noise (–160 dBm). The band 1559–1610 MHz, of which L_1 is a part, is allocated to Aeronautical Radio Navigation Services. GLONASS and Galileo also have allocations in this band.
(ii) GPS signals with the present power levels cannot readily penetrate into concrete and steel buildings or underground, and are susceptible to interference and jamming. The reflected signals (multipath) cause position errors.
(iii) Protection from the hostile use of GPS, while unaffecting the military user's PPS.
(iv) For civilian users, lack of signal redundancy to improve accuracy and availability.

To overcome these problems modernization of GPS is needed.

Conclusion

In this article, GPS system signal structure and frequency assignment are presented. Various error sources that cause the measured position inaccuracy are explained. The range measurement errors are attributed to several factors such as satellite ephemeris, clock, multipath, receiver noise and propagation delay of the satellite signals due to the ionosphere and troposphere. However, major error source results from the signal transmission through the ionosphere layers. This error can be dominant during periods of enhanced ionospheric activity. These periods of high ionospheric activity are usually accompanied by significant degradation of positioning accuracy, and degradation of receiver-tracking performance. GPS receiver data pertaining to the years 1998 and 2000 have been used and the solar activity has been very high during these years. High values of TEC are observed nearer to solar maximum year (2000–01). SVs with PRN no. 21 that travelled along 7°–11°N latitude experienced relatively high TEC values (35–80 TECu) than at low-latitude regions. One of the reasons for having relatively high TEC at 8° (80 TECu) than at 0° (20 TECu) could be due to the electrojet effect, which is common in the Indian subcontinent. To improve the signal redundancy, accuracy and availability, need for the introduction of additional GPS signals and M-codes on both the L_1 and L_2 frequencies is investigated.

1. Parkinson, B. W., *GPS Theory and Applications, Volume II*, American Institute of Aeronautics and Astronautics, Inc, Washington, 1996, pp. 81–114.
2. Ananda, M. P. and Chernick, M. R., High accuracy orbit determination of near earth satellites using Global Positioning System (GPS). In Proceedings of IEEE PLANS 82, IEEE PLANS (Atlantic City, NJ), Institute of Electrical and Electronics Engineers, New York, 6–9 December 1982.
3. Hofmann-Wellenhof, B., Lichtenegger, H. and Collins, J., *GPS: Theory and Practice*, Springer Wien, New York, 1997, 4th revised edn, p. 389.
4. Rizos, C., *Satellite Ephemeris Bias. Principles and Practice of GPS Surveying*, The University of New South Wales, Sydney, Australia, 1999.
5. Langley, R. B., The GPS observables. *GPS World*, 1993, **4**, 52–59.
6. Spilker, J. J., *Global Positioning System: Theory and Applications*, Progress in Astronautics and Aeronautics, 1996, vol. 163, pp. 517–546.
7. Hopfield, H. S., Two-quartic tropospheric refractivity profile for correction satellite data. *J. Geophys. Res.*, 1969, **74**, 4487–4499.
8. Saastamoinen, I., Contribution to the theory of atmospheric refraction. *Bull. Geod.*, 1973, **107**, 13–34.
9. Mendes, V. B., Modeling the neutral-atmosphere propagation delay in radiometric space techniques. Ph D thesis, University of New Brunswick, 1998, p. 353.
10. Klobuchar, J. A., *Global Positioning System: Theory and Applications*, Progress in Astronautics and Aeronautics, 1996, vol. 163, pp. 485–515.

Received 19 December 2006; revised accepted 3 August 2007